Investigation of the $^2S_{1/2}$-$^2D_{5/2}$ clock transition in a single ytterbium ion

P. Taylor,[1] M. Roberts,[1] S. V. Gateva-Kostova,[2] R. B. M. Clarke,[3] G. P. Barwood,[1] W. R. C. Rowley,[1] and P. Gill[1]
[1]*National Physical Laboratory, Queens Road, Teddington, Middlesex TW11 0LW, United Kingdom*
[2]*Institute of Electronics, boulevard Tsarigradsko Shausse 72, 1784 Sofia, Bulgaria*
[3]*Department of Physics and Applied Physics, University of Strathclyde, 107 Rottenrow, Glasgow G4 0NG, United Kingdom*
(Received 25 April 1997)

The suitability of the 411-nm $^2S_{1/2}$-$^2D_{5/2}$ transition in Yb^+ is assessed as an optical frequency standard. The lifetime of the $^2D_{5/2}$ level has been measured and found to be 7.2 ± 0.3 ms, which implies a natural linewidth of 22.2 ± 0.9 Hz for the 411-nm transition. In addition to a decay to the ground state the $^2D_{5/2}$ level can decay into the highly metastable $^2F_{7/2}$ level where it is trapped. The branching ratio for decay into the $^2F_{7/2}$ level has been measured and found to be 0.83 ± 0.03. A transition capable of rapidly depopulating the $^2F_{7/2}$ level and returning the ion to the cooling cycle has been demonstrated. This has enabled a quantum jump measurement of the 411-nm transition in $^{172}Yb^+$ to be performed, yielding a center frequency of 729 476 869.13(0.42) MHz (1σ). [S1050-2947(97)01710-1]

PACS number(s): 32.70.Cs, 06.30.Ft, 32.80.Pj, 42.50.Lc

I. INTRODUCTION

A forbidden transition, in a single laser-cooled ion stored in an electrodynamic trap, has significant potential as an optical frequency standard. It has been speculated that reproducibilities of 1 part in 10^{18} could be realized with this technique [1]. The use of a weak ''clock'' transition is desirable since its high Q leads to a standard with high stability. The detection of a weak transition is facilitated by the use of quantum jumps. Currently, many different ion species are being investigated to assess their suitability as standards, for example, Hg^+, Yb^+, Sr^+, Ca^+, and In^+ [2].

The ytterbium ion is the most versatile of the various ion species under consideration, having clock transitions in the visible, infrared, and microwave regions of the spectrum. The 171 isotope of Yb^+ is particularly promising as a reproducible standard, having levels with integer angular momentum and hence $m_F=0$ to $m_F=0$ transitions that are free from the linear Zeeman effect. In fact, this isotope has spin $\frac{1}{2}$, which is especially favorable as the overall atomic system has a minimal hyperfine structure, simplifying laser cooling. However, the work reported in this paper uses $^{172}Yb^+$, which has no hyperfine structure, which further simplifies the experiments.

The ytterbium ion has three candidate transitions in the optical spectrum. This paper assesses one of these transitions for its suitability as a standard. The 411-nm $^2S_{1/2}$-$^2D_{5/2}$ transition, shown in Fig. 1, was originally proposed by Werth [3]. However, on driving the transition [4] it was found that an ion in the $^2D_{5/2}$ state could decay to the extremely metastable $^2F_{7/2}$ level where it is trapped ''indefinitely.'' To overcome this difficulty the ion must be returned to the cooling cycle by driving a subsidiary transition. The demonstration of a suitable transition [5] has allowed the 411-nm $^2S_{1/2}$-$^2D_{5/2}$ transition to be investigated as an optical frequency standard.

Both of the other optical transitions under consideration as standards have recently been driven [6,7]. Notably, the 467-nm $^2S_{1/2}$-$^2F_{7/2}$ transition is the weakest feature in the optical spectrum, the $^2F_{7/2}$ level having a radiative lifetime of ten years [7]. Prior to its direct observation the location of this transition was established by measurements of the 3.43-μm $^2F_{1/2}$-$^2D_{5/2}$ interval [8] and the 411-nm $^2S_{1/2}$-$^2D_{5/2}$ interval (this work).

This paper reports three experimental results. In Sec. III two different transitions capable of depopulating the $^2F_{7/2}$ state are investigated. This allows quantum jumps at 411 nm to be observed, enabling a line profile for the transition to be taken. The observation of this line profile and a measurement of its center frequency is discussed in Sec. IV. To assess the suitability of the $^2S_{1/2}$-$^2D_{5/2}$ 411-nm transition as an optical frequency standard it is necessary to know the linewidth of the transition. This is deduced in Sec. V by measuring the lifetime of the $^2D_{5/2}$ state. This experiment also gave the branching ratios of the $^2D_{5/2}$ level for decay into the ground state and $^2F_{7/2}$ level.

II. EXPERIMENTAL ARRANGEMENT

A schematic layout of the apparatus used in the experiments described in this paper is shown in Fig. 2. A single ion of $^{172}Yb^+$ was confined in an electrodynamic (Paul) trap. The electrodes consist of a ring and two end caps. The ring diameter is $2r_0=1.00$ mm and the end-cap separation is $2z_0=0.94$ mm. An ac voltage of amplitude 350 V and frequency $\Omega=2\pi\times11.50$ MHz is applied to the ring to form a pseudopotential well in which the ion is trapped. In addition, a dc voltage of 18 V is applied to the ring, which modifies the axial and radial oscillation frequencies making them approximately equal $\omega_r\approx\omega_z=2\pi\times1.1$ MHz. If the ion is moved away from the ac center of the trap by a stray electric field it experiences additional micromotion at the drive frequency. This is corrected by applying a small dc voltage to one of the end caps. The success of this operation is gauged using the rf photon correlation technique [9]. The trap parameters and calculated minimum kinetic energy achieved by laser cooling predict that the ion will be confined in the Lamb-Dicke regime [10], eliminating the first-order Doppler

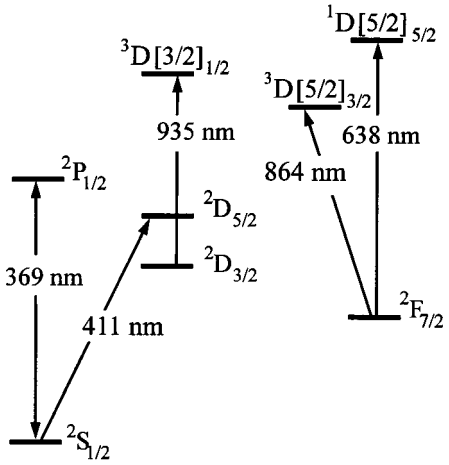

FIG. 1. Partial term scheme of Yb^+. The arrows show the transitions driven in these experiments.

effect. This was recently confirmed by observing the magnitude of the secular sidebands in the $^2S_{1/2}$-$^2F_{7/2}$ transition profile [7].

The ion is laser cooled by repeatedly driving the $^2S_{1/2}$-$^2P_{1/2}$ resonance transition at 369 nm, which has a natural linewidth of 19.6 MHz [11,12]. From the $^2P_{1/2}$ state there is a branching ratio of 0.66% [13] for decay into the metastable $^2D_{3/2}$ state. To maintain the cooling cycle, the $^2D_{3/2}$ state is rapidly depopulated by a laser at 935 nm [14], returning the ion to the ground state via the $^3D[3/2]_{1/2}$ level. The light at 369 nm is generated by an argon-ion pumped, frequency-doubled Ti:sapphire laser. Approximately 50 μW of light is focused into a 100 μm spot radius at the center of the trap. The frequency drift of the Ti:sapphire laser is reduced to about 100 kHz/min by locking it to a Burleigh confocal étalon. The 935-nm radiation is generated by a laser diode in an extended cavity. This produces around 10 mW of light with a linewidth of 2 MHz, which is focused to a 100 μm spot radius at the center of the trap. Single ion count rates of up to 50 kHz are observed.

The $^2S_{1/2}$-$^2D_{5/2}$ clock transition at 411 nm is driven by radiation from a frequency-doubled diode laser. The fundamental radiation is emitted from an SDL5420C diode mounted in a grating feedback system in the Littrow configuration. The grating has 1200 lines/mm, blased for a center wavelength of 250 nm. The laser diode produces up to 75 mW of 822-nm light, which is frequency doubled in an angle-tuned crystal of lithium triborate. The fundamental radiation is built up in an enhancement cavity. Up to 50 μW of radiation is produced with this system. The laser diode frequency is locked to the enhancement cavity using the Pound-Drever-Hall technique [15]. This reduces the laser diode linewidth to about 750 kHz. In the first instance long-term steering of the 411-nm light was provided by locking the 822-nm light to a confocal reference cavity of finesse 5. The error signal from this was applied to a piezomounted mirror in the enhancement cavity. This system reduced the frequency drift to about 1 MHz/min. For a measurement of the 411-nm transition frequency a further stage of long-term frequency stabilization was used, which is described in Sec. IV.

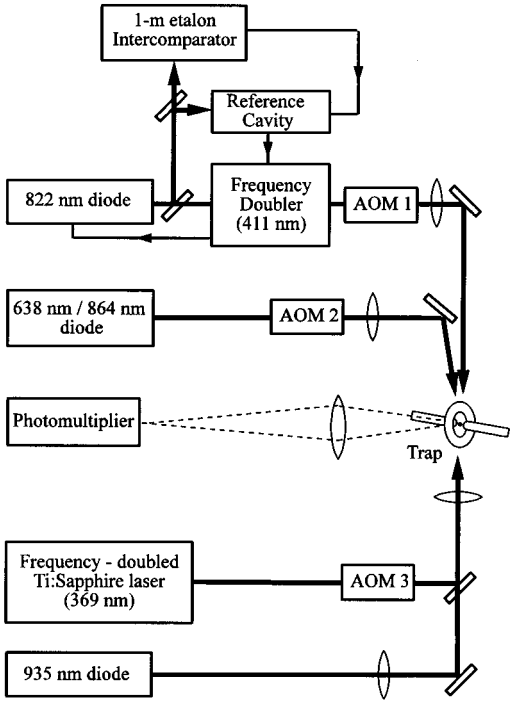

FIG. 2. Experimental layout.

III. COMPARISON OF $^2F_{7/2}$ LEVEL CLEAROUT LASERS

An ion driven into the $^2D_{5/2}$ state may decay either to the ground state or into the extremely metastable $^2F_{7/2}$ state, from where it is not observed to decay spontaneously. Therefore, in order to observe repeated quantum jumps of the $^2S_{1/2}$-$^2D_{5/2}$ transition it is necessary to rapidly depopulate the $^2F_{7/2}$ level with a further laser. Two transitions have been investigated for this purpose: $^2F_{7/2}$-$^1D[5/2]_{5/2}$ transition at 638 nm and the $^2F_{7/2}$-$^3D[5/2]_{3/2}$ transition at 864 nm (see Fig. 1).

To assess the effectiveness of these transitions, quantum jumps are observed in a single ion by simultaneously irradiating the ion with the cooling lasers, the 411-nm laser, and one of the $^2F_{7/2}$ level clearout lasers. The duration of the quantum jump ''off'' time measures how rapidly the ion is returned from the $^2F_{7/2}$ level to the cooling cycle. Both radiations were generated by laser diodes mounted in grating feedback extended cavities. An SDL-7501-G1 diode generated around 4 mW of 638-nm radiation. An SDL-5432-H1 diode generated about 20 mW of 864-nm light. Both lasers had an instantaneous linewidth of order 1 MHz with acoustic jitter of about 5 MHz. In both cases the light was focused onto a 150 μm spot radius at the center of the trap.

Figures 3 compares the best data obtained in both experiments. Clearly, the 638-nm laser is more effective, the off times being considerably shorter. This is quite a surprising result. The 638-nm transition is forbidden ($E2$) and the $^1D[5/2]_{5/2}$ level has $E1$ decays into the $^2D_{3/2}$ and $^2D_{5/2}$ states. These decays are not strong enough to be listed in the tables [13] nor are they seen in emission lamp spectra [16]. The 864-nm transition is also forbidden ($E2$); however, the $^3D[5/2]_{3/2}$ level has much stronger $E1$ decays into the $^2S_{1/2}$ and $^2D_{5/2}$ levels, which are seen in an emission lamp [16] and have calculated [13] oscillator strengths of 0.039 and

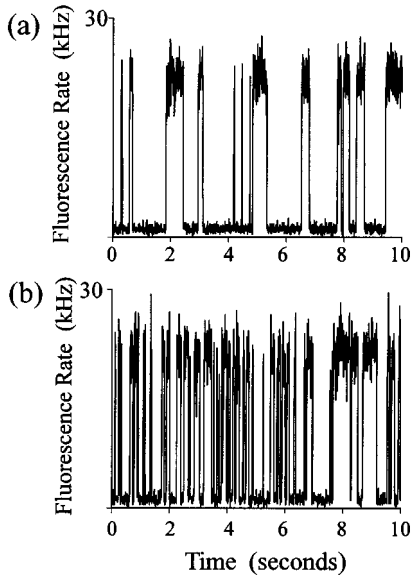

FIG. 3. Comparison of $^2F_{7/2}$ level clearout lasers: (a) the 864-nm laser and (b) the 638-nm laser. The duration of off periods is clearly shorter when the 638-nm laser is used, which indicates its greater efficacy.

0.011. The fact that the 638-nm laser is far more effective at restoring fluorescence, despite its inferior power, suggests that the $E2$ $^2F_{7/2}$-$^1D[5/2]_{5/2}$ transition is stronger than the $E2$ transition used by the 864-nm laser.

IV. MEASUREMENT OF THE $^2S_{1/2}$-$^2D_{5/2}$ TRANSITION FREQUENCY

A quantum jump profile of the $^2S_{1/2}$-$^2D_{5/2}$ transition was obtained by irradiating a single ion with the cooling lasers and the 638-nm laser while scanning the 411-nm laser frequency over the transition. The 411-nm frequency is measured by comparison with an iodine-stabilized He-Ne laser using a 1-m Fabry-Pérot étalon. This National Physical Laboratory étalon can be used to compare optical wavelengths with an accuracy of typically 1×10^{-10} [17,18].

The experimental arrangement is shown in Fig. 2. The light at 369 and 411 nm was chopped in antiphase by acousto-optical modulators (AOM1 and AOM3 in Fig. 2) to avoid broadening the narrow 411-nm transition. Light at 935 and 638 nm was on at all times. (The additional acousto-optical modulator AOM2 shown in Fig. 2 was not present during this part of the experiment.) A fluorescence rate of 15 kHz with a background of 3 kHz made it possible to set a threshold level such that an *on* or *off* state could be determined after a 5-ms cooling interrogation. At each frequency point of the 411-nm laser, 200 clock and cooling cycles were performed. If the ion underwent a transition to the $^2D_{5/2}$ level during the 10-ms clock pulse, then the subsequent cooling pulse detected no fluorescence; i.e., the ion was off, The clock cycle was then suspended until the fluorescence returned. The number of off jumps that occurred at each frequency point was recorded and the results plotted as a histogram. At the maximum jump rate only one in five clock pulses produced a transition. This low rate reduces the chance of the ion being driven off and on again during the clock pulse, which would distort the line shape.

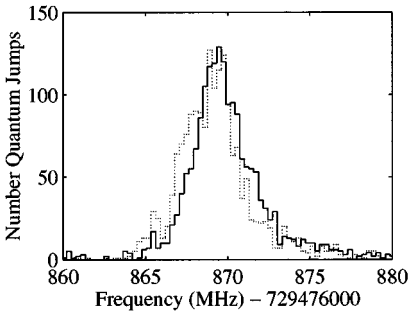

FIG. 4. Quantum jump profile of the $^2S_{1/2}$-$^2D_{5/2}$ transition. $\Delta m_J=\pm1$, magnetic field 29 μT. Solid line, decreasing frequency; dotted line, increasing frequency.

To obtain an absolute frequency calibration of the 411-nm scan, a portion of the fundamental light at 822 nm was locked to the peak of a 1-m étalon [17]. The error signal from the 1-m étalon transmission fringe was fed back to the diode laser's reference cavity. The étalon was locked to a scannable He-Ne laser, which was itself offset locked to an iodine-stabilized He-Ne laser. A knowledge of the étalon order number and the beat frequency between the two He-Ne lasers allowed an absolute frequency measurement of the 822-nm laser. The 822-nm light is frequency doubled and a shift of -60.000 MHz is applied with an acousto-optic modulator. The frequency of the 411-nm light was stepped by changing the beat frequency between the two He-Ne lasers, using a voltage controlled offset-lock unit. The lock between the 411-nm light and the 1-m étalon was poor, broadening the 411-nm linewidth to around 3 MHz. A series of scans were taken, each having a width of 23 MHz made up of 82 bins. As the frequency of the 411-nm laser did not drift, successive profiles could be added together to improve the statistics. In the data shown here each profile is the sum of four scans. Scans of the $^2S_{1/2}$-$^2D_{5/2}$ transition were taken in both frequency directions to check for any systematic shift.

The $^2S_{1/2}$-$^2D_{5/2}$ transition is made up of ten Zeeman components. To simplify the observed spectrum a small known magnetic field was applied to the ion to select only four of these components. In zero magnetic field the fluorescence rate falls to zero due to optical pumping into the $m_J=\pm3/2$ states of the $^2D_{3/2}$ level. This effect allows the magnetic field to be nulled to about ±1.5 μT, using three orthogonal pairs of field coils. A small controlled magnetic field was then applied. Two measurements of the transition were made. For the first a magnetic field of 29 ± 4 μT was applied, the direction of which selected the $\Delta m_J=\pm1$ Zeeman components. The splittings of the components are calculated to be ±325 and ±650 kHz, with relative intensities of $\frac{2}{3}$ and $\frac{1}{3}$, respectively. The result of these scans is shown in Fig. 4. In the second measurement a larger field of 130 ± 11 μT was applied; the direction of the field and the 411-nm laser polarization selected the $\Delta m_J=\pm2$ transitions. In this case the expected splittings are ±3.6 and ±5.1 MHz, with relative intensities of $\frac{5}{6}$ and $\frac{1}{6}$, respectively. This larger magnetic field allowed the Zeeman structure to be partially resolved (Fig. 5). The profile consists of two peaks of two components each. The expected intensity weighted splitting of 7.8 ± 0.7

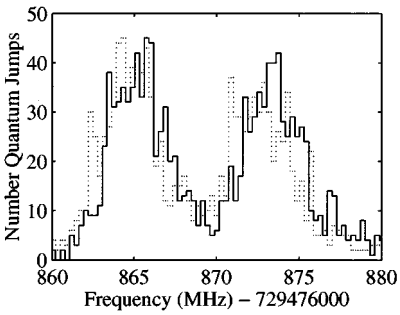

FIG. 5. Quantum jump profile of the $^2S_{1/2}$-$^2D_{5/2}$ transition. $\Delta m_J = \pm 2$, magnetic field 130 μT. Solid line, decreasing frequency; dotted line, increasing frequency.

MHz is in agreement with the measured splitting of 8.2 ± 0.3 MHz.

An examination of the profiles in Figs. 4 and 5 shows that there is a systematic shift that depends on the direction of the frequency scan. Splittings between the forward and reverse scans of 570 kHz (Fig. 4) and 850 kHz (Fig. 5) are observed. The direction of the shift is consistent with a lag caused by the slow nature of the servo loop used to lock the laser to the 1-m étalon. However, this systematic error is effectively controlled since both forward and reverse scans were taken. The data from the forward and reverse scans are analyzed separately and then their mean is taken to obtain the center frequency.

Both of the profiles show some asymmetry in the line shape, though this is particularly noticeable in the low field case (Fig. 4). The profile's ''tail'' is extended on the high-frequency side for both forward and reverse scans. The cause of this asymmetry is not properly understood. It is possible to estimate the size of the asymmetry by considering different horizontal ''slices'' of the data and taking the mean of each slice. From the difference in the means the asymmetry is estimated to be about 280 kHz.

Careful study of the high-magnetic-field line shape suggests that the low-frequency peak is slightly larger than the high-frequency peak. This is because the $m_J = -1/2$ state of the $^2S_{1/2}$ level is preferentially populated by laser cooling [19]. The orientation of the magnetic field and cooling laser polarization selects $\Delta m_J = \pm 1$ Zeeman components of the cooling transition. The cooling laser is positioned halfway up the low-frequency side of the transition. This drives the low-frequency component $^2S_{1/2}(m_J = +1/2)$-$^2P_{1/2}(m_J = -1/2)$ at a slightly higher rate than the high-frequency component. Therefore, the population of the $m_J = +1/2$ state is slightly more depleted than the $m_J = -1/2$ state.

The frequency measurement has three components: the determination of the center frequency of the scan range, the scan range calibration, and the determination of line center. The errors in determining the center of the scan range at 822 nm are summarized in Table I. The first seven errors arise in the interferometric comparison of the 822-nm light with the iodine stabilized HeNe [17]. The final error is the accuracy [20] of the I_2-HeNe. The errors are combined in quadrature to get the total error at 822 nm; consequently, the error at 411 nm is twice this value. The errors in the determination of the $^2S_{1/2}$-$^2D_{5/2}$ transition frequency are summarized in Table II. The error analysis presented is based on the low-magnetic-field data (Fig. 4). The first entry is the determination of the center of the scan range, which has just been discussed. The scale of the scan was determined by a calibration of the voltage-controlled offset-lock frequency. This calibration is good to 1% at 822 nm and hence to 2% at 411 nm. Since most of the data lie within about 3 MHz of the center of the scan, this error is therefore at most 60 kHz. The systematic shift of the center frequency in the direction of the scan is removed by completing scans in both directions. A 25% residual is assumed for the remaining uncertainty. The asymmetry in the line shape is the largest single error in the measurement. As already discussed, this is estimated to be about 280 kHz. Finally, there is a statistical uncertainty in the location of line center which is about 140 kHz.

TABLE I. Uncertainty in the 822-nm center frequency.

Source of uncertainty	Fractional error (10^{-10})
phase-shift determination	0.3
flatness and illumination uniformity	0.3
prismatic imbalance (image shear)	0.6
diffraction	0.2
servo errors	0.2
diffuser Doppler shift	1.4
statistical repeatability	2.9
633-nm accuracy	0.3
fractional error in 822-nm centre frequency	3.3

The mean frequency for the low-magnetic-field case is 729 476 869.13(0.42) MHz. This measurement therefore has a fractional accuracy of 6 parts in 10^{10}. The mean frequency for the high-field case is 729 476 869.00(0.50) MHz. The error bar on this second measurement is larger because of the slightly larger forward-reverse shift, an increased scan calibration error (the data are further from the center frequency), and an increased statistical error. The measurements are in excellent agreement both with each other and with the previous measurement of 729 476 868(11) MHz [21].

V. LIFETIME OF THE $^2D_{5/2}$ LEVEL

To assess the suitability of the $^2S_{1/2}$-$^2D_{5/2}$ transition as a frequency standard, it is important to know the lifetime of the $^2D_{5/2}$ level. This determines the linewidth of the transition and hence the maximum possible stability that could be achieved by the standard.

TABLE II. Total error in the $^2S_{1/2}$-$^2D_{5/2}$ transition frequency.

Source of uncertainty	Error (kHz)
411-nm center frequency	240
scan calibration	60
residual forward-reverse bias	140
line asymmetry	285
location of line center	140
total error in the $^2S_{1/2}$-$^2D_{5/2}$ transition frequency	420

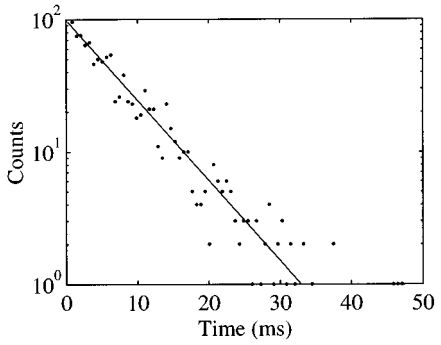

FIG. 6. Measurement of the $^2D_{5/2}$ level lifetime. Distribution of fluorescence off periods for decay from the $^2D_{5/2}$ level to the ground state (dots) and the weighted least-squares fit (line).

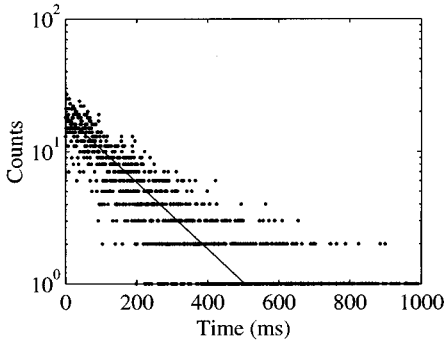

FIG. 7. Measurement of the time to return the ion to the cooling cycle from the $^2F_{7/2}$ level using the 638-nm laser. Distribution of fluorescence off periods (dots) and the weighted least-squares fit (line).

Measurements of the duration of the off periods in quantum jump data have been used to determine the lifetimes of many atomic states (e.g., [22,23]). The duration of the off periods in quantum jump data are governed by the lifetime of the metastable state. The distribution of the duration of off periods is an exponential function, with a decay rate equal to the reciprocal of the level's lifetime. In previous experiments of this type, an ion is placed in the metastable state by a pulse of light from the clock laser. Interrogation by the cooling laser determines when the ion decays back to the ground state. The distribution of off times then gives the lifetime of the state.

For Yb^+ this scheme is complicated due to the additional decay route of the $^2D_{5/2}$ level to the extremely metastable $^2F_{7/2}$ level. However, the two decay routes can be easily distinguished as an ion decaying to the $^2F_{7/2}$ level remains off for an indefinitely long period, provided no 638-nm light is applied. To make use of this fact the 638-nm laser is gated by an acousto-optic modulator (AOM2 in Fig. 2) such that the 638-nm light is only switched on 200 ms after fluorescence has disappeared (over 30 times the expected $^2D_{5/2}$ lifetime). The ion is prepared in the $^2D_{5/2}$ state by a 1-ms pulse of 411-nm light. The 369-nm light is then switched on to determine when the ion decays back to the ground state. A fluorescence rate of over 40 kHz, with a background of 0.5 kHz, ensured that in a 0.6-ms bin the ion could be reliably identified as being either on or off. If the ion *does* decay to the ground state, the bin in which the fluorescence resumed is recorded, giving the duration of the off event. If the fluorescence has not returned after 200 ms, the 638-nm laser is turned on until the ion returns to the cooling cycle. Recording the number of times the 638-nm laser was used to return the ion to the cooling cycle allows the $^2D_{5/2}$ level branching ratio to be determined.

Figure 6 shows a semilogarithmic plot of the first section of the off duration data, which is attributed to a direct decay from the $^2D_{5/2}$ level to the ground state. A weighted least-squares fit of these data to a single exponential yields a $^2D_{5/2}$ level lifetime of 7.2 ± 0.3 ms. Figure 7 shows a semilogarithmic plot of the second section of data, which is due to decays from the $^2D_{5/2}$ level to the $^2F_{7/2}$ level and then the subsequent depopulation by the 638-nm laser. An exponential fit to this data gives a ''lifetime'' of 172 ms; i.e., it takes 172 ms on average to return the ion to the cooling cycle once the 638-nm laser is turned on. The frequency of the 638-nm laser was not always exactly on resonance and needed to be adjusted occasionally during the experiment. These data therefore only provide an upper limit on the time to restore the fluorescence with the 638-nm laser.

Fawcett and Wilson's [13] theoretical estimate of 5.74 ms for the $^2D_{5/2}$ level lifetime compares reasonably with the measured value of 7.2 ± 0.3 ms. The experiment also measures the branching ratio of the $^2D_{5/2}$ level. In total 6183 jumps were observed, of which 1082 decayed to the ground state and 5101 were trapped in the $^2F_{7/2}$ level. This gives branching ratios of $A_{D\rightarrow F}/\Sigma A=0.83\pm0.03$ and $A_{D\rightarrow S}/\Sigma A=0.17\pm0.04$. The theoretical estimates compare well, being 0.803 and 0.197, respectively.

VI. CONCLUSION

The 411-nm $^2S_{1/2}$-$^2D_{5/2}$ transition has been investigated to assess its suitability as an optical frequency standard. The decay path of the $^2D_{5/2}$ level into the $^2F_{7/2}$ level necessitates the use of an additional laser to maintain the clock cycle. Two transitions at 864 and 638 nm have been investigated for this purpose, of which the 638-nm transition was found to be the more effective. The measurements reported here show that the 638-nm laser is able to return the ion to the cooling cycle in about 170 ms. If the frequency stability of the 638-nm laser were improved, it may reduce this time further. It is possible to observe rapid quantum jumps by using the 638-nm laser to depopulate the $^2F_{7/2}$ level. This makes the 411-nm $^2S_{1/2}$-$^2D_{5/2}$ transition into a viable spectral reference.

Repeated quantum jumps of the 411-nm $^2S_{1/2}$-$^2D_{5/2}$ transition has been observed. A quantum jump measurement of the $^2S_{1/2}$-$^2D_{5/2}$ transition frequency has been performed, giving a center frequency of 729 476 869.13(0.42) MHz. This measurement has an accuracy of 6 parts in 10^{10}.

The work reported in this paper uses the 172 isotope of ytterbium, which has no hyperfine structure. To make a frequency standard with good reproducibility it is desirable to use $^{171}Yb^+$ since this isotope has transitions free from the linear Zeeman effect. However, the presence of a hyperfine structure complicates laser cooling. It is hoped to overcome this difficulty in future work.

The lifetime of the $^2D_{5/2}$ level has been measured and found to be 7.2 ± 0.3 ms. In addition, the branching ratio of the $^2D_{5/2}$ level has been measured and found to be 0.83 ± 0.03 for decay into the highly metastable $^2F_{7/2}$ level. The theoretical predictions of both the lifetime and branching ratios are in reasonable agreement with the experimental results.

The lifetime of the $^2D_{5/2}$ level implies that the $^2S_{1/2}$-$^2D_{5/2}$ transition has a natural linewidth of 22.9 ± 0.9 Hz and therefore a $Q=3\times10^{13}$. The Allan deviation of a laser locked to this transition in a single ion using a 0.7-ms interrogation time would be [24] $\sigma_y(\tau)=8\times10^{-15}\tau^{-1/2}$, making it acceptable as a high-stability frequency reference.

ACKNOWLEDGMENTS

S.V.G.-K. was financially supported by the Royal Society/NATO. R.B.M.C. acknowledges financial support from the EPSRC. The authors would like to thank S. N. Lea for a critical reading of the manuscript and H. A. Klein for his many helpful discussions.

[1] H. Dehmelt, IEEE Trans Instrum. Meas. **31**, 83 (1982).
[2] *Proceedings of the Fifth Symposium on Frequency Standards and Metrology*, edited by J. C. Bergquist (World Scientific, Singapore, 1996).
[3] G. Werth, Metrologia **22**, 190 (1986).
[4] H. A. Klein *et al.*, IEEE Trans Instrum. Meas. **40**, 129 (1991).
[5] P. Gill *et al.*, in *Proceedings of the Fifth Symposium on Frequency Standards and Metrology* (Ref. [2]), pp. 159–164.
[6] C. Tamm and D. Engelke, in *Proceedings of the Workshop on Frequency Standards Based on Laser Manipulated Atoms and Ions*, edited by J. Helmcke and S. Penselin (PTB, Braunschweig, 1996), Vol. PTB-Opt 51, pp. 45–50.
[7] M. Roberts *et al.*, Phys. Rev. Lett. **78**, 1876 (1997).
[8] A. S. Bell *et al.*, J. Mod. Opt. **39**, 381 (1992).
[9] R. Blümel, C. Kappler, W. Quint, and H. Walther, Phys. Rev. A **40**, 808 (1989).
[10] R. H. Dicke, Phys. Rev. **89**, 472 (1953).
[11] R. W. Berends, E. H. Pinnington, B. Guo, and Q. Ji, J. Phys. B **26**, 701 (1993).
[12] R. M. Lowe, P. Hannaford, and A.-M. Mårtensson Pendrill, Z. Phys. D **28**, 283 (1993).
[13] B. C. Fawcett and M. Wilson, At. Data Nucl. Data Tables **47**, 241 (1991).
[14] A. S. Bell *et al.*, Phys. Rev. A **44**, R20 (1991).
[15] R. W. P. Drever *et al.*, Appl. Phys. B **31**, 97 (1983).
[16] W. F. Meggars, C. H. Corliss, and B. F. Scribner, *Tables of Spectral-Line Intensities, Part I Arranged by Elements*, 2nd ed., Natl. Bur. Stand. (U.S.) Monograph 145 (U.S. GPO, Washington, DC, 1975).
[17] G. P. Barwood *et al.*, Phys. Rev. A **43**, 4783 (1991).
[18] G. P. Barwood, W. R. C. Rowley, and P. T. Woods, Metrologia **20**, 157 (1984).
[19] G. P. Barwood *et al.*, Appl. Phys. B **61**, 385 (1995).
[20] T. J. Quinn, Metrologia **30**, 523 (1993).
[21] P. Gill *et al.*, Phys. Rev. A **52**, R909 (1995).
[22] W. Nagourney, J. Sandberg, and H. Dehmelt, Phys. Rev. Lett. **56**, 2797 (1986).
[23] W. M. Itano, J. C. Bergquist, R. G. Hulet, and D. J. Wineland, Phys. Rev. Lett. **59**, 2732 (1987).
[24] D. J. Wineland *et al.*, in *Proceedings of the Fourth Symposium on Frequency Standards and Metrology*, edited by A. De Marchi (Springer-Verlag, Berlin, 1989), pp. 71–77.